13

The Generation and Characterisation of Ultrashort Mid-Infrared Pulses

J. Biegert[1,2], P.K.Bates[1] and O.Chalus[1]
[1]*ICFO – Institut de Ciencies Fotoniques*
[2]*ICREA – Institució Catalana de Recerca i Estudis Avançats*
Spain

1. Introduction

Over the past decade, ultrashort pulsed light sources have become an indispensable tool both in the laboratory and over a wider range of applications in the medical, industrial and telecommunication sectors. The availability of energetic sub-100 fs pulses, combined with the stability and usability of solid-state laser amplifiers, has opened up entire new fields such as femtochemistry, laser micro-drilling and knife-less laser eye surgery. However, while current ultrashort pulse sources are highly developed, their central wavelengths almost exclusively lie in the near-infrared spectral range below 1000 nm.

Specifically, coherent pulses of mid-infrared (mid-IR) radiation, i.e. at wavelengths longer than 3 microns, are intensely sought for a range of applications in the life sciences, spectroscopy and environmental sensing but have not readily been available due to various technical challenges. These challenges are related not only to detecting and handling mid-IR radiation but also to the scarcity of mid-IR sources. Much effort has been invested in developing appropriate sources and technology to enable reliable production of such sources, but, even 50 years after the invention of the laser, a large portion of the mid-IR spectrum remains inaccessible, especially if one is interested in ultrashort pulsed sources. It is just within the last years that optical technology has made a major step forward; recent advances in fiber technologies are becoming available and reliable nonlinear media are now accessible. However, the current generation of mid-IR sources is not yet nearly as advanced as those in the near-IR. The various approaches and techniques often cover very narrow spectral ranges, come with very low output power, or are unable to provide short pulses of radiation. The last point in particular is common to the majority of mid-IR sources commonly used to date. Another drawback is that these very specific sources are typically designed as a specialists tool for a particular application. Very few systems have been designed to offer a robust, all-round performance in a flexible, upgradeable format. Thus, mid-IR sources often lack flexibility, and, with each source optimised for a very narrow set of applications (or perhaps even just one application), mid-IR source development has fractured into different specialist areas, resulting in a lack of coherence across the field, and ultimately thwarting the advancement of mid-IR science and technology.

In this chapter we will restrict ourselves to sources of ultrashort pulses in the mid-IR spectral range. We will begin by motivating the development of sources as well as some technical limitations, mention some available sources as well as describe our new platform

for ultrashort pulses and describe why it promises to even surpass the performance of the current state-of-the art NIR systems.
The range of applications of such a mid-IR source is immense, particularly in bio-medical and biological research. Figure 1 shows a compilation of information relative to these fields, absorption curves of tissue and water as well as absorption bands of molecules which constitute the building blocks of life.

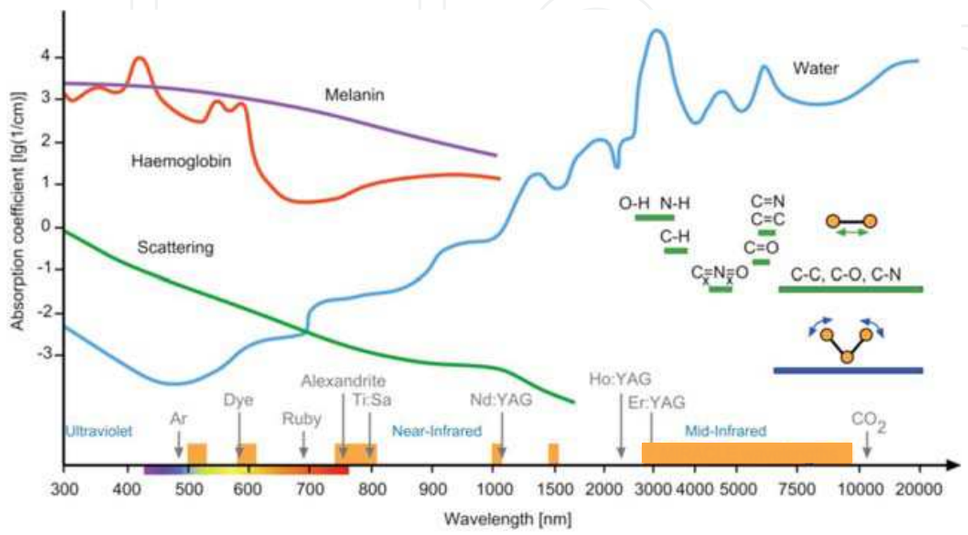

Fig. 1. Shown are common (long pulse) laser sources and the wavelength range accessible in the mid-IR by the system described in this chapter. Overlaid are the the absorption curves and scattering in tissue together with major absorption bands of marker molecules and compounds of interest; adapted from Peng et al. (2008)

Figure 1 clearly demonstrates that, while visible wavelengths are more suitable for imaging applications, due to a longer penetration depth, mid-IR wavelengths hold a clear advantage in terms of selectivity and rapid (and localized) absorption. In fact, femtosecond lasers can function as a pair of nano-scissors in sub-cellular surgery and have potential applications in a single organelle or chromosome dissection, inactivation of specific genomic regions on individual chromosomes and highly localised gene and molecular transfer. The major advantage of pulsed laser nano-surgery is the well-controlled and non-invasive capability of severing sub-cellular structures with high accuracy in time and three-dimensional space.
Spectroscopy of cellular compounds or volatile components in human breath will have its highest sensitivity and selectivity in the mid-IR since those wavelengths cover most of the molecular absorption bands and since each molecule or compound has its specific fingerprint. By closely monitoring the spectral shifts or changes in line strength, it will become possible to see how those compounds behave in their environment. Ordinary human breath is teeming with bio-molecules that can reveal the presence or absence of certain diseases or metabolic processes. To date, researchers have identified over 1000 different compounds contained in human breath that have both endogenous and exogenous origins, and provide information about physiological processes occurring in the body, as well as environment-related ingestion or absorption of contaminants. Just as bad breath can indicate dental problems, the identification and measurement of molecules in exhaled breath can provide a window into the metabolic state of the human body. While the

presence and concentration of many of these molecules are currently not well understood, many biomarker molecules have been correlated to specific diseases and metabolic processes. Such correlations provide the potential for non-invasive methods of health screening for a wide variety of medical conditions, including detecting the presence of cancer, monitoring respiratory diseases, assessing liver and kidney function, and determining exposure to toxins. For example: excess methylamine may signal liver and kidney disease; ammonia may be a sign of renal failure; elevated acetone levels can indicate diabetes; and nitric oxide levels may be used to diagnose asthma. More sensitive, earlier detection of disease is obviously highly desirable in all cases, but in many conditions this can spell the difference between life and death.

While many of the above-mentioned applications can be covered by continuous wave or long-pulse sources, some applications will significantly benefit from ultrashort pulsed sources. This can be due either to the fact that shorter pulses usually go hand in hand with high achievable intensities, as required for nanosurgery applications, or to the pulse's broad spectral bandwidth, which allows easy detection over many absorption bands instead of arduous scanning. In particular, high intensities and well controlled electrical fields are the basic requirement for investigations in fundamental strong field physics, when the laser electric field strength approaches that of the atomic binding energy in the matter. Almost all such investigations are extremely sensitive to the electric field structure of the laser pulse, require high repetition rates due to the low probability of the processes under investigation, and are particularly sensitive to the wavelength of the driving laser.

Many strong field physics experiments involve the measurement of photoionised electrons, which makes mid-IR pulses very interesting, since they allow for a much clearer discrimination between tunnelling and multi-photon ionisation, whereas current ultrashort NIR laser sources operate in a mix of multi-photon and tunnelling ionisation regimes. The lower photon energy of mid-IR pulses can be used to create strong field experiments that clearly involve tunnelling ionisation only, allowing investigation of fundamental atomic processes with unprecedented clarity.

Another growing area of interest is the production of attosecond (10^{-18}s) pulses from ultrashort intense femtosecond lasers. Attosecond pulses with a carrier frequency corresponding to extreme ultraviolet wavelength can be produced from short-pulse laser systems, using high order harmonic generation (HHG) as coherent up-shifting mechanism from the near-IR drive laser (Mcpherson et al. (1987); Ferray et al. (1988)). The availability of few-cycle mid-IR light pulses for this purpose should yield shorter attosecond pulses due to a square of wavelength dependence of the shortest wavelength reachable via HHG (Sheehy et al. (1999); Gordon and Kaertner (2005)). Recent experiments have confirmed this scaling of the harmonic cutoff with drive wavelength, while showing that predicted losses in harmonic yield (Tate et al. (2007)) can be compensated by taking advantage of more favourable HHG phase matching at longer wavelengths (Popmintchev et al. (2008)). Based on their results we expect a 3 μm source to generate harmonic spectra extending to a photon energy well above 1 keV.

A unique feature of the source we present here is its ability to operate at extremely high repetition rates. Higher repetition rates help to improve signal to noise ratio for most experiments, but they are also essential for some in strong field physics; for instance, particle coincidence experiments with reaction microscopes (COLTRIMS) (Moshammer et al. (1996)) permit the investigation of atomic and molecular processes with unprecedented scrutiny, but are limited mainly by the stability of current lasers due to the low cross sections of the processes under investigation; the measurement time is, in practice, nearly always longer

than the time over which the best lasers can deliver constant performance. Using a 100 kHz repetition rate, experiments taking six days with a 1 kHz system can be completed in 90 min, greatly reducing the demands on the laser system stability.

Many of the demands of strong field physics are extremely challenging for any laser system. In particular, the generation of single attosecond pulses requires driving pulse durations of only a few cycles of the underlying electric field, and a stable carrier-to-envelope phase (CEP). The CEP is the offset between the peak of the pulse intensity envelope and the peak of the underlying electric field, as shown in Fig. 2. For a pulse whose duration is many cycles of the electric field, this parameter is relatively unimportant, but for a few-cycle pulse such as the one shown in Fig. 2, the structure of the electric field can vary strongly with the CEP value, and can adversely affect an experiment. CEP stability is therefore necessary to maintain the electric field shape between successive laser pulses, and is a considerable technical challenge for even the most advanced systems.

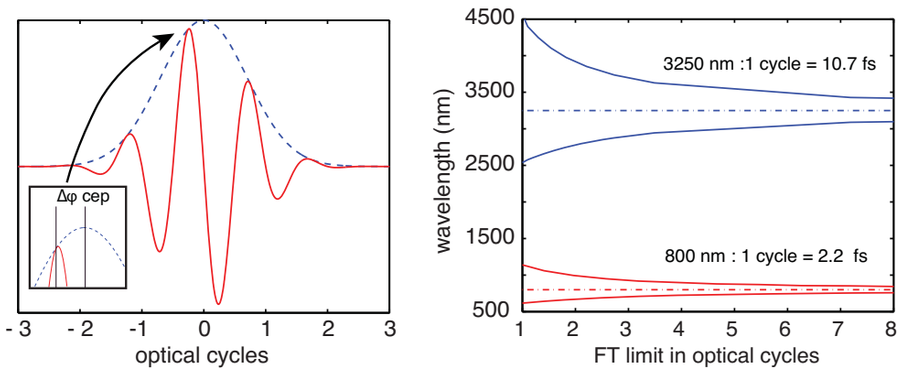

Fig. 2. The left panel shows the intensity envelope (blue, dashed) and electric field structure (red, solid) of a few-cycle pulse, with the definition of the carrier envelope phase shown in the inset. The CEP must be controlled to ensure the electric field structure is constant from pulse to pulse. The immense bandwidth needed to support such a few-cycle pulse is shown in the right panel, for pulses centered at 800 nm (red) and 3250 nm (blue), plotted against pulse duration in optical cycles.

Current high-energy feedback stabilised systems are capable of CEP locked operation for several hours at most. Total CEP stability of the laser source is essential for many experiments, both in attoscience measurements which typically involve large scans of pump-pulse delay times, and even more so for photoionisation experiments. For example, the measurement of double ionisation demands CEP stability over about 12 hours with a 1 kHz repetition rate; an unrealistic requirement from current electronically stabilised systems. As we will see in the following sections, moving central wavelengths to the mid-IR allows us to use a method of passive CEP stabilisation that has been proven to operate with no slow drifts over >240 hours. Finally, generating ultrashort pulses in the mid-IR necessarily requires the generation of large bandwidths, with few-cycle mid-IR pulse spectra covering hundreds of nanometers – the bandwidths of pulses at 800 and 3250 nm are shown in Fig. 2, normalised to the pulse duration in optical cycles. These spectra have the ability to cover simultaneously many vibrational transitions in important molecules, and this combined with the intrinsic potential CEP stability opens a wide range applications (Thorpe and Ye (2008)). Generating and amplifying such a bandwidth requires careful management of dispersion throughout the laser system, in a wavelength range where many materials

have anomalous dispersion, poorly characterized dispersion curves or limited transmission bandwidth. Control of the bandwidth and spectral phase is essential for few-cycle pulse generation, as is an accurate method of pulse characterisation.

2. Few-cycle mid-IR pulse generation

The development of any ultrashort pulsed source in the mid-IR should not only match but ideally surpass the abilities of current NIR sources. State of the art pulse durations at centre wavelengths in the visible to NIR currently lie in the few-cycle range at repetition rates up to several kHz. Sources are nearly exclusively based on Ti:Sapphire chirped pulse amplification (CPA) systems, combined with spectral broadening via gas-filled hollow fibres (Nisoli et al. (1998)) or filamentation (Hauri et al. (2004)) and compression in the visible to near-IR (NIR) with chirped mirrors (Schenkel et al. (2003)) to routinely generate pulses with durations of a few cycles of the electric field. These systems are intrinsically limited to the NIR by their reliance on Ti:Sapphire CPA, and as such cannot be directly reproduced in the mid-IR. The way to access ultrashort pulses in the mid-IR proceeds nearly exclusively via three wave mixing in nonlinear crystals and specifically parametric amplification to overcome the limited gain bandwidth of Ti:Sapphire or other solid state gain media.

We would like here to distinguish between optical parametric amplification (OPA) and optical parametric chirped pulse amplification (OPCPA) approaches, even though, strictly speaking, all sources of ultrashort pulses are OPCPA due to the near impossibility of avoiding chirp. The distinction is made therefore by labelling OPA as an approach without intended and pre-defined chirp in contrast to OPCPA where the seed pulse to be amplified has to acquire a pre-defined chirp. This distinction is nevertheless important, as OPA based approaches are limited in energy due to the high peak powers of the pump pulse used in the process.

Probably the most established method to access ultrashort mid-IR pulses is via non-collinear OPA of some white light continuum or frequency shifted output, from Ti:Sapphire (Wilhelm et al. (1997)) or, more recently, Yb-based fiber CPA systems (Schriever et al. (2008)). For the broad spectra of hollow fibre broadened Ti:Sapphire lasers DFG can also be used (Vozzi et al. (2006)), followed by amplification in an OPA using the Ti:Sapphire system as a pump. Different implementations of these various approaches have generated few-cycle pulses at 1.2 – 3 μm (Vozzi et al. (2006); Cirmi et al. (2008); Zhang et al. (2009)) and recently this has been extended to longer wavelengths, delivering 25 fs duration pulses at ~ 3 μm, with pulse energies of 2 μJ (Brida et al. (2008)). The latter system amplifies a white-light continuum with a Ti:Sapphire pump laser to generate an amplified signal at 1.3 μm. In a second stage OPA this signal is amplified further, and the idler from the interaction is extracted, which has 2 μJ infrared energy at 3 μm. The CEP stability of this system has yet to be proven, and scaling to higher energies is limited by the un-chirped nature of the OPA interaction, however it is an interesting source of low energy mid-IR pulses. The low energy output from such frequency converted systems is very applicable to ultrafast spectroscopy, where it has found many uses (Nibbering and Elsaesser (2004)).

Mixing of amplified ultrashort pulses from a Ti:Sapphire laser with longer pulses at around 1 μm wavelength has been shown to produce ultrashort pulses in the mid-IR (Sheehy et al. (1999); Rotermund et al. (1999)), but is limited to roughly the duration of the driving laser pulse, and suffers from low efficiency. This technique has been a workhorse of ultrafast mid-IR spectroscopy, but is unlikely to be scalable to higher energy or few-cycle pulse durations, and does not provide CEP stable pulses.

A more exotic, but elegant, approach to few-cycle mid-IR pulse generation (Fuji et al. (2006)), uses a four wave mixing process generated inside a filament in air. The interaction of the 800 nm fundamental of a Ti:Sa system and its second harmonic results in an 13 fs 1.3 cycle pulse with 1.5 μJ energy at a wavelength of 3.4 μm and extremely broad bandwidth. However, this system has poor efficiency, requiring 1.8 mJ of fundamental to generate just over 1 μJ. Moreover, the repetition rate is low at 1 kHz, and the stability of such a system is unclear. Furthermore the scalability is inherently limited to μJ energies due to the intensity clamping in the filament, which limits the pump energy to ~1 mJ for ~ 30 fs pulses.

2.1 OPCPA in the mid-IR

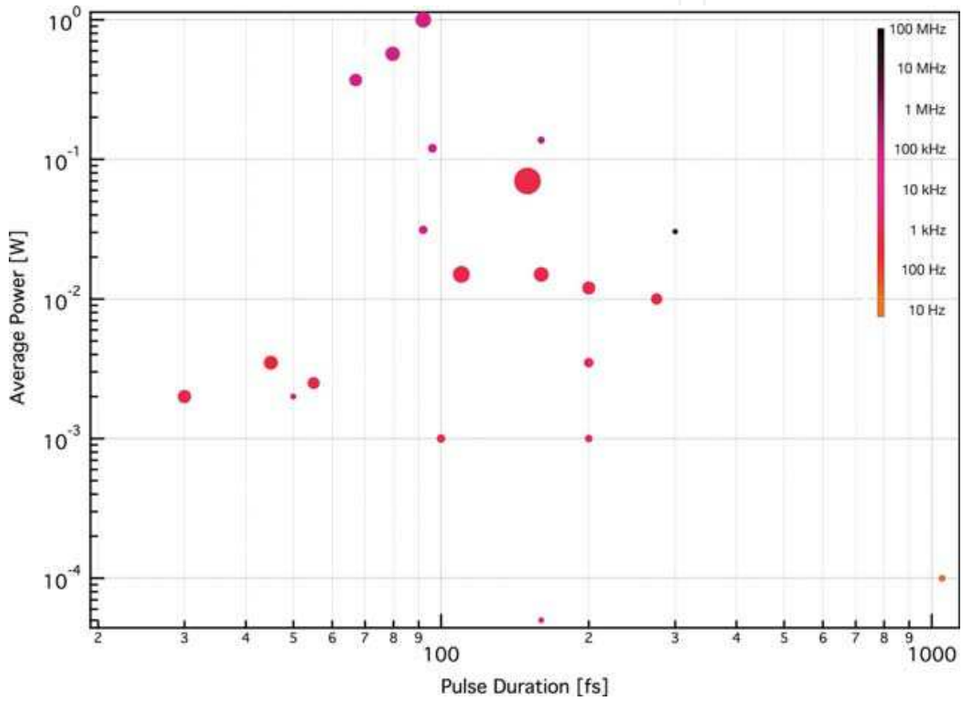

Fig. 3. **Mid-IR ultrashort pulse sources.** A summary of the ultrashort pulses available in the mid-IR. The colour scale represents repetition rate, while the size of each circle corresponds to the energy per pulse. The system described in this chapter lies in the top left quadrant of the picture.

An alternative approach to frequency-shifting of NIR laser systems is direct amplification of ultrashort mid-IR pulses using optical parametric chirped pulse amplification (OPCPA). OPCPA involves the amplification of broad-bandwidth chirped seed pulses using a narrowband, typically pico-to-nanosecond pump laser. This approach allows amplification across a huge range of central wavelengths in the NIR and mid-IR with ultra-broad gain bandwidths that make possible the direct amplification of few-cycle pulses. Indeed, NIR OPCPA sources have demonstrated that they can directly produce amplified few-cycle pulses as short as 5.5 fs (Adachi et al. (2008)). OPCPA systems have already been reported at 2.1 μm (Fuji et al. (2006)) and in the mid-IR at 3.2 μm (Chalus et al. (2009)).

Unlike the gain-storage media used in traditional CPA amplifiers, no energy is deposited in OPCPA, meaning that the possible pulse repetition rates are limited only by available pump

laser technologies. In contrast to OPA based schemes, OPCPA uses a long pump and chirped seed pulse, allowing the energy of the systems to be scaled up even to joule level energies (Chekhlov et al. (2006); Lozhkarev et al. (2006)). The previous two references are NIR OPCPA systems pumped by the second harmonic of the pump laser, and so moving to the mid-IR where pumping with the fundamental is possible should already increase the output energies. OPCPA is the only technology that currently offers the possibility of scaling up ultrashort mid- IR pulse energies to the Joule level.

2.2 OPCPA pump laser selection

OPCPA fundamentally is a nonlinear three-wave mixing process, and as such requires adequate (high) pump intensities to generate gain in reasonable crystal lengths. We can identify three main regimes for such pump sources: femtosecond, picosecond and nanosecond. Thus, a significant challenge is the selection of an appropriate pump laser for the OPCPA process.

Femtosecond systems with significant pump pulse energy typically employ CPA. The advantage of such an approach is that an OPCPA could serve as a back-end to simply extend the CPA's wavelength regime. The significant drawback is a highly complex system which inherits any problem that the CPA system might already have. Additional issues that one might have to address are the synchronisation between pump and seed over long path lengths as well as short pump pulses which could be beneficial in terms of achieving high pulse contrasts but as well limiting achievable efficiency.

Nanosecond durations are easily available from well developed pump sources, especially Q-switched Nd:YAG sources. Such lasers are very simple and reliable but their nanosecond duration requires very large seed stretch factors to be efficient in OPCPA. Especially the recompression to few-cycle pulse duration is far from trivial and could come with penalties in achievable contrast. Injection seeding or some form of synchronization of such Q-switched lasers is required due to their large pulse to pulse jitter. They typically also require longer crystal lengths to achieve significant gain, which can limit the bandwidth. However, nanosecond systems can produce energies orders of magnitude greater than femtosecond systems for a similar price.

Picosecond systems present a good compromise in terms of readily achieving pump pulse intensities for OPCPA whilst requiring moderate seed stretch factors and avoiding the complexity of CPA based pumps. Master-oscillator power-amplifier (MOPA) pump lasers with picosecond duration are commercially available in a wide range of configurations, with excellent performance characteristics and at repetition rates up to a few hundred kHz. These higher repetition rates can increase signal to noise ratios in experiments, and reduce data collection times, but only if the laser stability is not degraded by the increased repetition rate. As we have mentioned before, OPCPA as a technique is virtually repetition rate insensitive as no energy is deposited in the crystals, however, the pump laser's stability has a direct influence on the stability of the OPCPA, such that this parameter becomes extremely important. For example, during investigation of the change of absorption in a material as in (Gertsvolf et al. (2008)) fluctuations over a few percent already limited the measurement. As of today, OPCPA sources have achieved stabilities from 1.5% and higher (Tavella et al. (2010); Ishii et al. (2005)) while solid state lasers perform on a better level.

It should be noted that recent developments in high repetition rate and high energy fibre laser systems offer an interesting option for pumping OPCPA systems. These systems typically offer only a few hundred microjoules of energy but operate at repetition rates of a

few hundred kHz (Roser et al. (2005)) or even MHz repetition rates (Boullet et al. (2009)). These systems allow the use of small stretch factors in the OPCPA chain, and their low energy means that the short pulse duration does not lead to unreasonable requirements for large crystal apertures. They do offer the possibility of extremely high average powers, and more importantly near alignment-free OPCPA systems.

3. Experimental implementation of a mid-IR OPCPA source

In the remainder of this chapter we will describe an implementation of the sort of mid-IR ultrashort pulsed source motivated by the applications described in the introduction. The source has been designed to provide an extremely stable, high repetition rate pulsed source, with stable CEP, and capability for few cycle durations. In this implementation we have not explored the high energy capability of mid-IR OPCPA, but the possibility of upgrading the source is there, simply through the addition of extra amplifier stages. The source is compact, stable, easy to operate and we believe this approach leads to a source that can fulfil the key criteria needed across a wide range of applications in biology, spectroscopy, and strong field physics.

3.1 Generation of a CEP stable mid-IR seed pulse

There are currently no available broadband oscillators operating in the mid-IR, and thus the seed pulse for our system must be generated from a shorter wavelength oscillator and a nonlinear process. This in fact is very advantageous for a ultrashort long wavelength system, as it allows us to use a combination of standard, well-developed oscillator technology, and also to passively stabilise the CEP via difference frequency generation (DFG).

By mixing pulses with central wavelengths of 1050 nm and 1550 nm in an appropriate nonlinear crystal, a pulse can be generated via DFG at 3200 nm central wavelength. This pulse is the idler of the three wave mixing interaction, and the phase of the pump, signal and idler pulses (ϕ_p,ϕ_s & ϕ_i) in the interaction can be expressed as the following

$$\phi_s = \phi_s(0) - \frac{\Delta k z}{2} + \frac{\Delta k \gamma_s^2}{2} \int \frac{\mathrm{d}z}{f + \gamma_s^2} \tag{1}$$

$$\phi_p = \phi_p(0) - \frac{\Delta k}{2} \int \frac{f \mathrm{d}z}{1 - f} \tag{2}$$

$$\phi_i = \phi_p(0) - \phi_s(0) - \pi / 2 - \frac{\Delta k z}{2} \tag{3}$$

Where $\Delta k = k_s + k_i - k_p$ is the wave-vector mismatch, $\phi_x(0)$ is the input phase of the pulses, f is the fractional depletion of the pump energy, γ is a gain coefficient dependent on the crystal parameters, and z is the crystal length. In the case of perfect phasematching $\Delta k = 0$, the expression becomes simply

$$\phi_s = \phi_s(0) \qquad \phi_p = \phi_p(0) \qquad \phi_i = \phi_p(0) - \phi_s(0) - \pi / 2 \tag{4}$$

If the pump and seed pulses in the interaction originate from the same laser oscillator, they will have the same, although rapidly changing, CEP value. In the DFG interaction, the

difference between $\phi_p(0)-\phi_s(0)$ is therefore constant, and the idler phase is passively stabilised to a constant value. This principle has been successfully demonstrated experimentally (Baltuska et al. (2002)), and allows locking of the CEP phase to a fixed value with much less complexity than active-feedback systems commonly used in e.g. Ti:Sapphire oscillator systems. The effect of imperfect phasematching is to couple the output CEP to fluctuations in the pump laser intensity via the *f* parameter, but for a stable pump laser and a correctly aligned OPA this does not affect the CEP stability in a drastic way (Renault et al. (2007)).

In our experimental realisation, the seed for our OPCPA system is derived from a two-color fibre laser system (Toptica Photonics) which delivers amplified and phase-coherent ultrashort pulses at 1050 nm (48 fs, 16 mW) and 1550 nm (75 fs, 180 mW). The use of fibre laser ensures excellent timing stability between the two arms, alignment free and hands-off operation over long operation times. To generate the required ultrabroad mid-IR seed pulse, we use a difference-frequency generation (DFG) stage: DFG between the frequency shifted pulses from the fibre system allows generation of a seed pulse in the mid-IR spectral region which in our case stretches from 3000-4000 nm at the $1/e^2$ level. This configuration should passively stabilise the CEP of the generated idler pulses as described above, and measurements using the same fibre oscillator have shown timing jitter between the two arms to be less than 21 as over 200 hours, corresponding to a CEP drift of less than 90 mrad over this time, without complicated locking electronics or feedback loops (Adler et al. (2007)). There is also no need for octave spanning oscillators nor seed bandwidths and as a consequence complexity is reduced significantly.

DFG is achieved with a simple, 2 mm long, periodically poled lithium niobate crystal (PPLN) which yields a sub-picosecond duration mid-IR pulse with a spectrum covering 400 nm of bandwidth at the FWHM level with a power of about 1.5mW at 100MHz, corresponding to a transform limited pulse duration of 33 fs (Fig. 4). The PPLN crystal is poled in a fan-out geometry to allow fine-tuning of the phasematching bandwidth; the spatial variation of the fan-out poling is however chosen to vary slowly enough in order to avoid noticeable spatial chirp across the generated mid-IR beam. In order to preserve the CEP of the optically stabilized seed pulse, care must be taken with the system design. The entire OPCPA is enclosed in an air-tight insulated box, with a beam height of just 63 mm chosen to minimise mechanical vibrations of the mounts. The optics are mounted on 25 mm diameter stainless steel pedestals for optimum stability. The consideration of the CEP

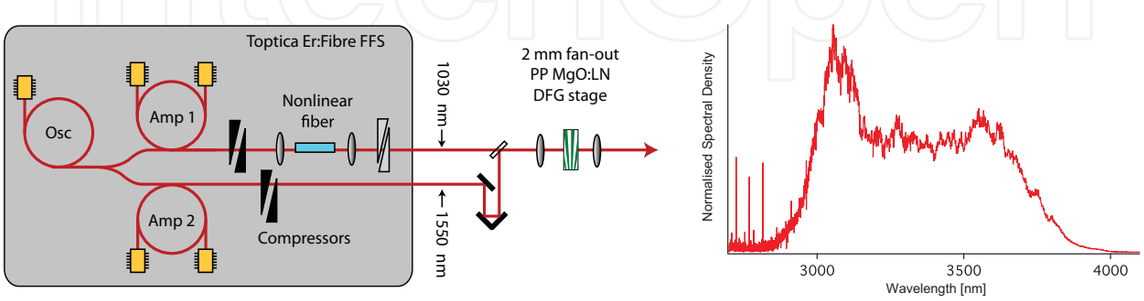

Fig. 4. **Mid-IR seed generation.** The two colour output from a commercial fiber MOPA system (FFS, Toptica Photonics) generates, via DFG, self-CEP stable, 3.2 μm radiation.

stability also defined our choice of stretcher system, as reports in the literature have identified the sensitivity of CEP stabilised systems to mechanical drifts in grating based stretcher or compressor systems. As such we prefer to use bulk stretching in a block of sapphire to avoid sensitivity to these drifts. Simulations of the DFG output show that the mid-IR pulse is already negatively chirped (Chalus et al. (2008)) to approximately 200 fs duration, and that a 5 cm long block of undoped Sapphire is sufficient to further negatively stretch the pulse to 6 ps compared to the pulse duration of 9 ps.

The stretched pulse duration must be a significant fraction of the pump pulse duration for good energy extraction, however, in high gain OPCPA stages the temporally varying intensity of a gaussian pump pulse can cause reduced gain for the edges of the chirped seed spectrum. A balance needs to be found between the pulse stretching and the effect on the bandwidth (Moses et al. (2009)). By modelling the relationship between gain and stretched pulse duration in our system, we have found that a combination of different stretched pulse durations in our amplifiers is the best configuration for our system. Because we are using a bulk stretcher, we can easily split the stretching into three separate stages, allowing the use of a short 1 ps stretched pulse in the first amplifier to optimise bandwidth and the cost of only a small reduction in energy extraction, while stepping up the pulse duration to 4 ps in the second and 6 ps in the third amplifier, where the low gain has less effect on the spectral width, and good temporal overlap allows efficient energy extraction. The stretched mid-IR seed pulse is difficult to characterise temporally, and we estimate the ratio between the pump duration and seed duration by changing their timing overlap in the first OPCPA stage and monitoring the spectral shift and idler energy.

The pump laser used for the OPCPA is a picosecond high-average-power pump laser from Lumera Laser GmbH. It operates at 1064 nm with 100 kHz at 40W output power and with pulse duration of 8 ps. Its spatial mode is close to $M^2 \approx 1.2$ and it has stability better than from the most advanced Ti:Sa CPA systems; power fluctuations of <0.4% pulse–to–pulse and <0.1% RMS over 15 hrs are *routinely* observed. The fiber oscillator is used as master oscillator and the pump laser's oscillator is slaved to it to better than 350 fs rms over 6 hours via an electronic synchronization unit (Menlo Systems). As will become evident for the results we present for this system, the timing jitter between the pump and seed pulses does not prevent the generation of extremely stable mid-IR pulses. (Chalus et al. (2009))

For optimum stability, mid-IR OPCPA systems should make use of optical synchronization of pump and seed pulses, such as that used in (Teisset et al. (2005); Fuji et al. (2006)). While electronic stabilisation systems have worked well here and in other OPCPA systems (Witte et al. (2005)), passive optical stabilisation offers a simpler, more robust way to cleanly synchronise the pump and signal pulses without drift for many hours. It is particularly easy in the mid-IR, where the long wavelength of the seed pulse means that the frequency shifting needed to seed the pump laser is towards higher frequency, which is usually easier to achieve and more efficient than shifting to lower frequencies.

3.2 The OPCPA amplification chain

The OPCPA amplifier chain in our system (Fig. 5) consists of three OPCPA stages, each configured for a different gain level. The choice of three stages allows us to optimise bandwidth, stability and energy extraction: by using the first stage to generate high gain with little depletion of the pump, the second stage to slightly deplete the pump and the final stage run well into pump depletion, we can take advantage of the fact that a strongly

depleted OPCPA amplifier shows approximately linear coupling between pump intensity fluctuations and amplified seed fluctuations (Ross et al. (2007)). Using a nearly-depleted and depleted stage in series ensures that over a reasonable range of pump laser fluctuations we can stay in the optimum range of depletion to maximise the seed stability. The use of a three stage OPCPA system also allows us to increase the amplified bandwidth by tuning the first and second crystals to amplify slightly different parts of the spectrum. This does reduce the total output of the system somewhat, but allows us to increase bandwidth by nearly 100 nm.

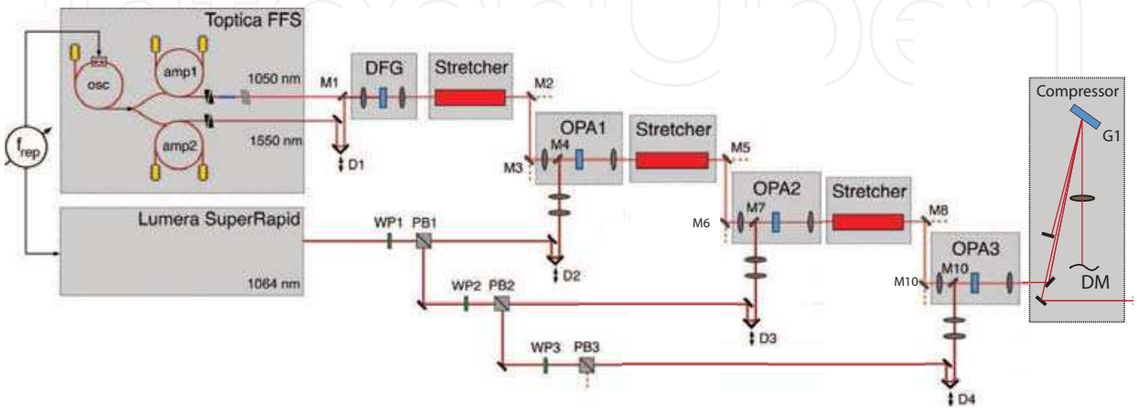

Fig. 5. **Mid-IR OPCPA source layout.** The two colour output from a commercial fiber MOPA system (FFS, Toptica Photonics) generates, via DFG, self-CEP stable, 3.2 μm radiation. These pulses are then stretched and amplified by a triple stage OPCPA pumped by a Nd:YVO_4 laser (SuperRapid, Lumera Laser) and finally compressed by a Martinez-type compressor. The compressor includes a linear deformable mirror with which we fine tune dispersion.

The operating parameters for the first stage are crucial since the highest gain is achieved here. We refrain from operating at maximum possible gain in order to achieve a good balance between amplification and parametric fluorescence background. The seed-pump spatial ratio is set to ~ 3 : 2. The first stage is a 2 mm fan-out periodically poled MgO:LN crystal pumped at an intensity of 60 $GWcm^{-2}$, giving an energy gain of 8×10^3, close to the small signal gain value calculated at 1.1×10^4. The pump power of 2.1W at 100 kHz results in an amplified idler at 3.2 μm centre wavelength, (note that our seed is the idler wave) with a bandwidth of 200 nm FWHM and approximately 80 nJ energy. (Fig. 6). The extraction efficiency of <1% into the idler is low due to the small pump-signal overlap in time and low

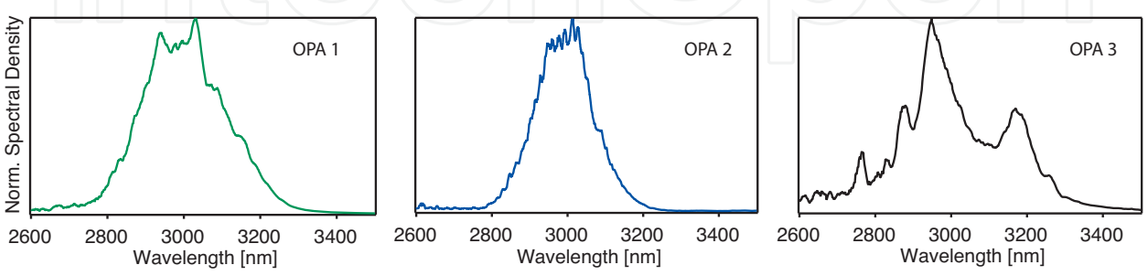

Fig. 6. **The amplified mid-IR spectra after each OPA stage in the system**. The first OPA is biased slightly towards shorter wavelengths, while the amplification in the second and third OPA broadens the spectrum and shifts it to longer wavelengths

depletion, however operating such a high gain stage with a longer chirped pulse of 6 ps led to a reduction in the amplified bandwidth of 50 nm. In any case, the three-stage design does not require high efficiency in this first stage.

The second OPCPA stage uses a crystal identical to the first, pumped with 5.1W average pump power to give a pump intensity of 57 $GWcm^{-2}$. The seed pulse is propagated from the first to the second stage collimated, using dielectric mirrors and filters to reject the residual pump light and amplified signal from the first OPA at 1550 nm. It passes through the second 1 cm sapphire block to stretch the duration to 4 ps, allowing for more efficient energy extraction without affecting the bandwidth. The energy gain in the second amplifier is 40, leading to an amplified idler energy of 1.2 μJ, and and amplified spectrum of 250 nm bandwidth FWHM centered at slightly longer wavelength than the first stage.

The amplified seed pulse from the second OPCPA stages is again filtered by dielectric filters, and passes through the third sapphire block to give a pulse duration of 6 ps as the final amplifier seed. The final OPCPA stage is again an identical crystal pumped at the same intensity of ~ 55GW/cm^2, but uses 20Wof average power to generate over 1Wof amplified idler power. This corresponds to 10 μJ per pulse in the idler centered at 3.1 μm, a conversion efficiency of 5% which however compares well to other OPCPA systems when the quantum efficiency of the process is taken into account. The combination of an idler at 3.1 μm, a signal at 1.5 μm and a pump at 1 μm means that the signal:idler photon ratio should be approximately 3:1. The conversion efficiency of 5% therefore implies a total of 5+10=15% conversion into the signal and idler from the pump, and is not unreasonable for a broadband OPCPA system pumped by a gaussian spatial and temporal profile pump. These values correspond to the optimum energy configuration for the OPCPA system, but the bandwidth can be increased as mentioned above, by altering the tuning of the second and third stage. By optimising for a maximum bandwidth of 350 nm FWHM, the power drops to 550 mW or 5.5 μJ.

Parametric super-fluorescence has been observed to be a problem from previously reported OPCPA systems (Tavella et al. (2005)) and it is vitally important to minimise it in any OPCPA setup. To test the parametric superfluorescence of our system, we employed two different techniques. Simply blocking the seed, we measured the power output of the full OPCPA chain with all pumps set to their operational values. Alternatively, we could use the electronic synchronization to delay the seed relative to the pump by 20 ps-5 ns, so that no amplification was observed, but any long timescale radiation that might seed a parasitic process was still preserved. In both cases, no measurable fluorescence was observed in the reflectivity bandwidth of our dielectric mirrors, which runs from 2.8-3.6 μm. In fact, even when running with gold-coated mirrors, no measurable or visible fluorescence could be seen from the amplifiers. The dynamic range of this measurement is approximately four orders of magnitude. We attribute this to a careful choice of low small signal gain in the amplifiers, careful filtering between the amplifiers, and the cleanliness of our pump laser in space and time. The low parametric fluorescence is a particularly important feature of our system, as previous ultrashort OPCPA systems have shown decreased pulse contrast on a long timescale due to excessive parametric superfluorescence in the system (Tavella et al. (2005))

3.3 Pulse compression

The amplified idler pulse from the system is negatively chirped, and as such requires a positive dispersion compression system. As mentioned before, a non-grating based or bulk compressor is preferable to ensure the best CEP stability, but at our mid-IR wavelength this

type of compressor is difficult to implement. Transmissive materials with appropriate dispersion in the mid-IR such as Silicon or Germanium exhibit high refractive index and high absorption (on the order 3200 cm^{-1}), making their use energetically costly even if Fresnel losses are removed with proper coatings. For power-scaling of these systems, bulk compressors can become extremely costly, and show thermal effects due to their high absorption. In contrast, a relatively simple solution is to use a Martinez-type grating based system, similar to the stretchers typically employed in the visible to near-IR range.

Gold gratings with 200 l/mm are both cheap and readily available, and are appropriate for compression in this system, while due to the slow change in refractive index across our bandwidth in the mid-IR, CaF2 lenses can be used to create the imaging optics. Such a system is easily scaleable to higher power levels. As mentioned before, grating based systems are not ideal for CEP stabilised systems, however the sensitivity scales inversely with wavelength and is further reduced for large line spaced gratings, meaning that for our system should exhibit less CEP variation due to the compressor than NIR Ti:Sa systems. Many of these NIR grating compressor systems have been successfully CEP stabilised (Kakehata et al. (2004)) and yield performance similar to that of prism-based compressor systems.

Controlling the dispersion across the full 400 nm window of our pulse bandwidth is highly challenging, and we have chosen to use a programmable dispersive system to enable fine control of the spectral phase. To achieve this, we have placed a 1D deformable mirror with a silver-coated membrane (OKO Technology) in the Fourier plane of the 4-f compressor setup. It operates with 19 actuators and provides a maximum displacement of 9 μm which corresponds to a delay of about 60 fs or a phase of 12π our wavelength range. Each actuators's range is discretized in 4096 steps of about 2 nm addressed individually. The mirror is computer controlled and its optimum configuration was obtained by the use of a genetic algorithm to converge to the shortest pulse.

The final compressor setup uses two 200 line/mm gold coated gratings and a M=-1 telescope created by two 2" diameter 250 mm focal length CaF2 lenses, with the deformable mirror used to fold the compressor in the Fourier plane between the lenses. The compressor is designed to support 600 nm spectral bandwidth and exhibits a measured transmission efficiency of 70% for our current 350 nm bandwidth FWHM. Second order phase is solely adjusted through its grating separation with the deformable mirror operating passively without any deformation; minimum achievable pulse durations were measured to 85 fs.

To optimise the pulse duration, we measure the SHG conversion efficiency of the compressed pulse and compare it to that of the uncompressed one. This gives an extremely rapid feedback on the compressed pulse intensity, while ensuring the measurement is independent of any pulse intensity variations. The algorithm considered a population of 60 individuals, crossover and mutation were included and we took care that no excessively steep gradients were applied to neighboring actuators across the membrane. In our case the spectrum was spread over approximately 8 actuators only and convergence was achieved after about 180 generations.

Just measuring the SHG intensity not adequate for characterising the resulting pulse duration, and we therefore use our FROG measurement device, which will be described in the following section, to fully characterise the temporal electric field of the pulse. Figure 7(a) shows a FROG measurement of the shortest pulses obtained with the above-mentioned procedure and (b) and (c) the retrieved temporal profile and spectrum. The shortest measured pulse duration is 67 fs with the transform limit supporting 57 fs, while the compressed energy at the output of the system for the shortest pulse was 3.8 μJ. We believe the discrepancy can be assigned to a

number of factors: firstly, the use of SHG conversion efficiency as the feedback to the genetic algorithm limits the discrimination between different pulse durations and may not provide an adequate guide to finally remove all spectral phase errors. An alternative is to first optimize the SHG, then use feedback via the measured pulse duration of the FROG. This provides a very strong criteria for the genetic algorithm, but is significantly slower. Additionally, the dispersed spectrum covers only 8 actuators in the current system, and changing the lenses of the compressor would allow this to be extended to cover more actuators, hence a more accurate addressing of the spectral phase.

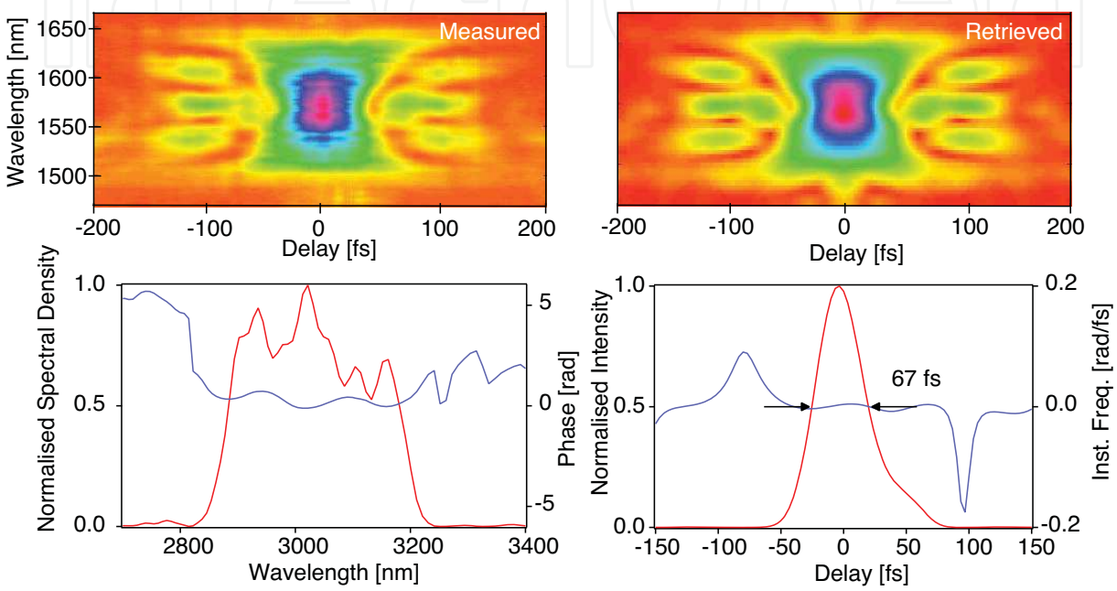

Fig. 7. Measured and retrieved SHG FROG traces of the compressed pulse (FROG Error =0.41%). Left: the measured FROG and retrieved spectrum and spectral phase.
Right: the spectra after each nonlinear stage.

4. Mid-IR pulse characterisation

To use few-cycle pulses in any experiment, full and accurate characterisation of the pulse is essential, and measurement of e.g. just the temporal intensity of the pulse is not adequate. Techniques such as auto-or cross correlation can provide limited information, and for clear understanding and control of the pulses we require a measurement that resolves the temporal electric field structure of the pulse, such as frequency resolved optical gating (FROG) (Trebino (2000)) and spectral phase interferometry for the direct reconstruction of electric fields (SPIDER) (Iaconis and Walmsley (1998)). Below we describe a SHG-FROG characterization device for mid-infrared pulses, optimised for measurement of true few-cycle (< 20 fs) mid-IR pulses. It has a working bandwidth of 1000 nm, can resolve femtosecond timescale structures over a temporal range of 100 ps and does not suffer from time reversal ambiguity as is seen with other SHG-FROG systems. The detector allows us to have high spectral resolution and the combined system enables measurement of few-cycle to picosecond durations without reconfiguration.

Characterisation of pulses at centre wavelengths up to 2 μm is relatively straightforward using standard techniques but at longer wavelengths, e.g. in the mid-IR, characterisation

becomes increasingly arduous. Array detectors are either unavailable, expensive, or come at very low resolution and require cryogenic cooling. Optics have to be carefully chosen to provide accurate response to the immense bandwidths; note that a 2 cycle pulse at 650 nm is associated with a $1/e^2$ bandwidth of 251 nm whereas it is 1212 nm at 3200 nm. While dispersion is low at 3 μm wavelengths, it contributes significantly to few-cycle pulses and has to be taken account of in the system design.

To date there have been several successful implementations of techniques to measure the full temporal electric field of ultrashort mid-IR pulses. The XFROG technique has characterized 13 fs mid-IR pulses (Fuji and Suzuki (2007)), however it requires a well synchronized ultrashort, precisely characterised laser pulse to use as a gate. Free-space electro-optic sampling (Grischkowsky et al. (1990)), also requires a synchronised shorter sampling pulse, which would have a duration of sub-10 fs if we used this technique at ~ 3 μm. For frequency converted Ti:Sa systems these pulses are often available, but with OPCPA the pulses would have to be generated through a complex frequency shifting process, and we may prefer a self-referencing technique such as polarisation-gating (PG-) or second-harmonic generation (SHG-) FROG, and SPIDER (Naganuma et al. (1989); Trebino (2000); Iaconis and Walmsley (1998)). SPIDER is suited for rapid acquisition (Kornelis et al. (2003)) whereas FROG has a simpler experimental arrangement and a wider temporal range. PG-FROG is unsuitable due to the finite response time of the nonlinear medium (Delong et al. (1995)) which limits its application for few-cycle pulses. SHG-FROG is suitable for those pulses (Akturk et al. (2004)); it can also cover a wide range of wavelengths and time durations, and is sensitive enough to be used with low energy pulses.

Temporal characterisation of a mid-IR FEL has been demonstrated via SHG-FROG (Richman et al. (1997)) for a 2 ps pulse with a small spectral width of ~40 nm, and a 25 fs OPA at 3.2 μm (Brida et al. (2008)). We present here a system whose range extends past both these pulse durations, while also operating over a wide range of central wavelengths.

The setup (Fig. 8) consists of only a Michelson interferometer and measures just 30×30 cm, for maximum stability and easy transportation. We use a pellicle beam splitter (Thorlabs) with negligible dispersion and a constant splitting ratio over the bandwidth, and a retroreflector mounted on a high resolution scanning stage (New Scale Technologies). All reflective optics are gold-coated to preserve the broad bandwidth. The stage can scan 15 mm with a resolution of 20 nm, corresponding to a time delay of 100 ps with 0.12 fs resolution. The corner cube gives a fixed lateral offset for a non-collinear, background free FROG signal

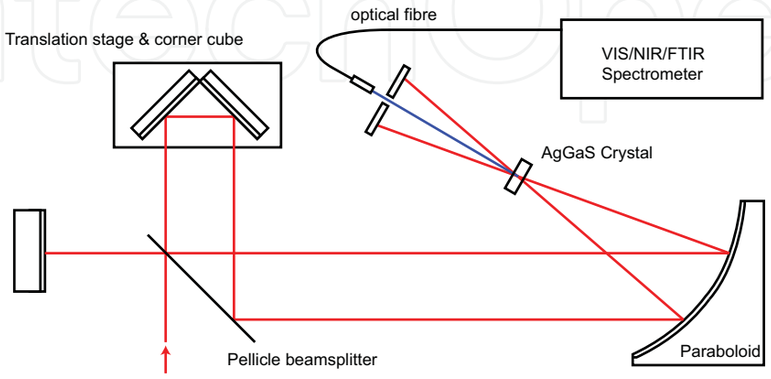

Fig. 8. **Layout of the SHG-FROG system** for mid-IR ultrashort pulse characterisation (see text).

while preventing any unwanted beam offset during long range scans. The two parallel output beams are focused with a 50mm focal length, off-axis parabolic mirror into the nonlinear crystal. The resulting non-collinear SHG is selected by an iris and coupled to a spectrometer via an optical fiber. This setup gives us the flexibility to measure broad bandwidths over a wide spectral range, with large high resolution time scans allowing accurate detection of pre- or post-pulses at picosecond delays, while simultaneously detecting a well-resolved femtosecond main pulse. Note that, even though this setup lends itself to single-shot measurements - at least up to 3500 nm fundamental wavelength - with InGaAs cameras, we refrain from doing so since the temporal dynamic range would be severely hampered by the SHG-FROG beam imaging geometry.

Crystal	Transparency Range (nm)	θ (deg)	d_{eff} (pm/V)	$\Delta\theta$ (mrad)	$\Delta\lambda$ (nm)
Ag_3AsS_3	600-13000	19.4	23.4	103.5	1100
$AgGaGeS_4$	700-13000	57.3	17.21	328	3400
$AgGaSe_2$	710-18000	76.5	35.1	1230	865
$AgGaS_2$	500-13000	35.7	9.11	312.5	2350
Ag_3SbS_3	700-14000	39.5	14.1	112	424
$Li:NbO_3$	330-5500	57.0	3.68	230.5	565
KTA (Type II e-axis)	330-4000	64.4	2.6	270	635

Table 1. Characteristics of SHG crystals at 3200 nm with 200 μm thickness. Data calculated with SNLO (Smith (2009)) θ is the phasematching angle, $\Delta\theta$ is the angular acceptance and $\Delta\lambda$ is the acceptance bandwidth following Smith (2009).

Table 1 shows a compilation of nonlinear crystals with a transparency range covering the fundamental as well as SH wavelengths, a suitably high d_{eff} for efficient conversion, and preferably Type I phase-matching to simplify the experimental layout. A pulse duration of 15 fs, or 1.5 cycles at 3 μm, requires a gaussian spectrum of ~1 μm FWHM, so we need to have substantially more than this to avoid strong spectral reshaping during SHG. A thin crystal is therefore warranted to support such immense bandwidths, but with the trade-off of reduced conversion efficiency. For a spot size of 35 μm, a five-cycle pulse with as low energy as 1 nJ results in an intensity of 1 GW/cm^2; this is sufficient to generate an adequate SH signal. We also need to accommodate a non-collinear angle of 100 mrad and an angular content due to focussing of 20 mrad for each of the generating beams.

KTA will phase-match in type II, and is limited by its transparency range and bandwidth, while neither the Ag_3AsS_3, $AgGaSe_2$, Ag_3SbS_3, nor the $Li:NbO_3$ have acceptance bandwidths that support few-cycle pulses. $AgGaGeS_4$ and $AgGaS_2$ (Silver Thiogallate) support a few-cycle pulse bandwidth, have adequate angular acceptance for our focussing geometry and a broad transparency range. The higher d_{eff} and broader bandwidth of the $AgGaGeS_4$ appears to make it a better candidate, however this crystal is not readily available, and so we resort to using $AgGaS_2$.

By exchanging the fibre-coupled spectrometer and crystal, we can use our FROG for 0.4-5 μm central wavelengths, with a Si-detector based spectrometer (Ocean Optics HR 4000) for SHG signals from near-IR radiation from 200-1100 nm, an InGaAs spectrometer (Ocean optics NIR 256) for SHG from 1000-2500 nm and a Fourier Transform Infra Red spectrometer (FTIR) (Oriel MIR8025) for 0.9-10 μm. The first two spectrometers provide quick response times, while the FTIR can measure over very large spectral ranges with extremely high resolution of up to 0.5 cm^{-1}. The spectrometers and motorised stage are

controlled through a home-built LabView program, which also reconstructs the pulse duration from the SHG-FROG trace using the PCGPA algorithm on a grid with sizes of up to 2048 x 2048 points. Such a large grid is necessary not only to measure and to retrieve with high enough resolution and to prevent aliasing but also to converge with a meaningfully small FROG error.

The first test measurement (Fig. 9) shows a richly featured mid-IR pulse from our OPCPA system. The center wavelength is at 3200 nm, the pulse energy is 1.2 μJ and its spectrum covers about 600 nm. We scanned the delay stage in steps of 6 fs, over a range of 3 ps, corresponding to 500 points of delay with a step size of 1 μm. High spectral resolution was ensured by the FTIR spectrometer, which recorded and summed 20 spectra at each delay point, sampled at a resolution of 1 cm^{-1}. To remove the SHG-FROG time ambiguity, we insert an 8 mm Silicon plate in the beam path and observe the sign of the phase change.

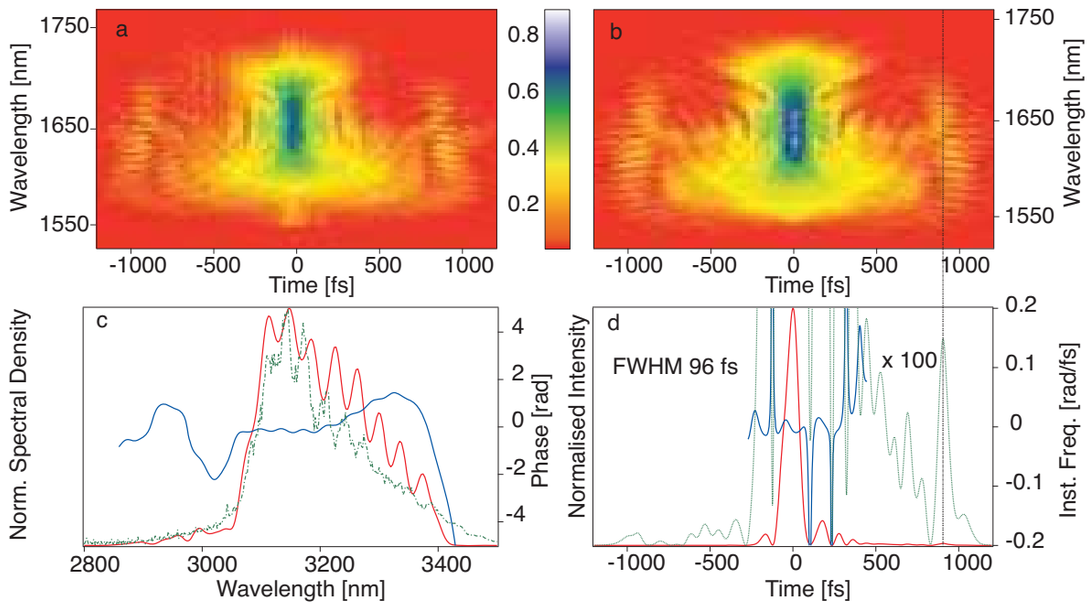

Fig. 9. **(a)**Measured FROG trace at 3.2 μm- colour shows the square root of intensity **(b)** Retrieved FROG trace. **(c)** Retrieved (solid) & measured (dotted) spectrum and phase. **(d)** Retrieved temporal pulse – also shown magnified ×100 (dotted) to highlight the well-resolved post pulse at 900 fs

Figure 9 a) shows the measured FROG trace with many complex femtosecond features across a >2 ps timescale. The long scan range and excellent signal to noise ratio ensures the detection of the post pulses at ~1 ps, while the high resolution FTIR captures the corresponding spectral fringes. The low intensity features of the trace are both detected and retrieved accurately as shown in Fig. 9 b). In contrast, a measurement with the low-resolution InGaAs spectrometer captures neither the post pulse nor the fringing. Reconstruction with high spectral and temporal resolution requires the use of a large grid size (2048x2048), and we achieve excellent agreement, with FROG error 0.0025. The retrieved pulses have a duration of 96 fs, corresponding to 9.0 cycles at 3.2 μm, and these pulses cover a 45 fs, 4.2 cycle transform limited bandwidth (Fig. 9 c) and d).

As a further test we measured a ~100 fs duration and 3.2 μJ energy pulse, centered at 3250 nm, before and after passing through a 1 cm thick sapphire plate. The delay stage was scanned in 400 steps of 6 fs for the directly measured pulse, and in 500 steps of 13 fs for the one with added dispersion; while integrating over 6 spectra for each delay point. Figure 10 a) & b) show the measured FROG traces, Fig. 10 c) & d) show the retrieved temporal profiles and instantaneous frequency, while Fig. 10 e) & f) show the reconstructed spectrum and spectral phase. The plate adds negative dispersion, and increases the retrieved pulse duration from 110 fs to 153 fs. We have calculated the expected phase for the pulse propagated through the sapphire, by adding the calculated phase of the sapphire to the retrieved phase of the undispersed pulse. This is plotted as a dotted line in Fig. 10 f), and we

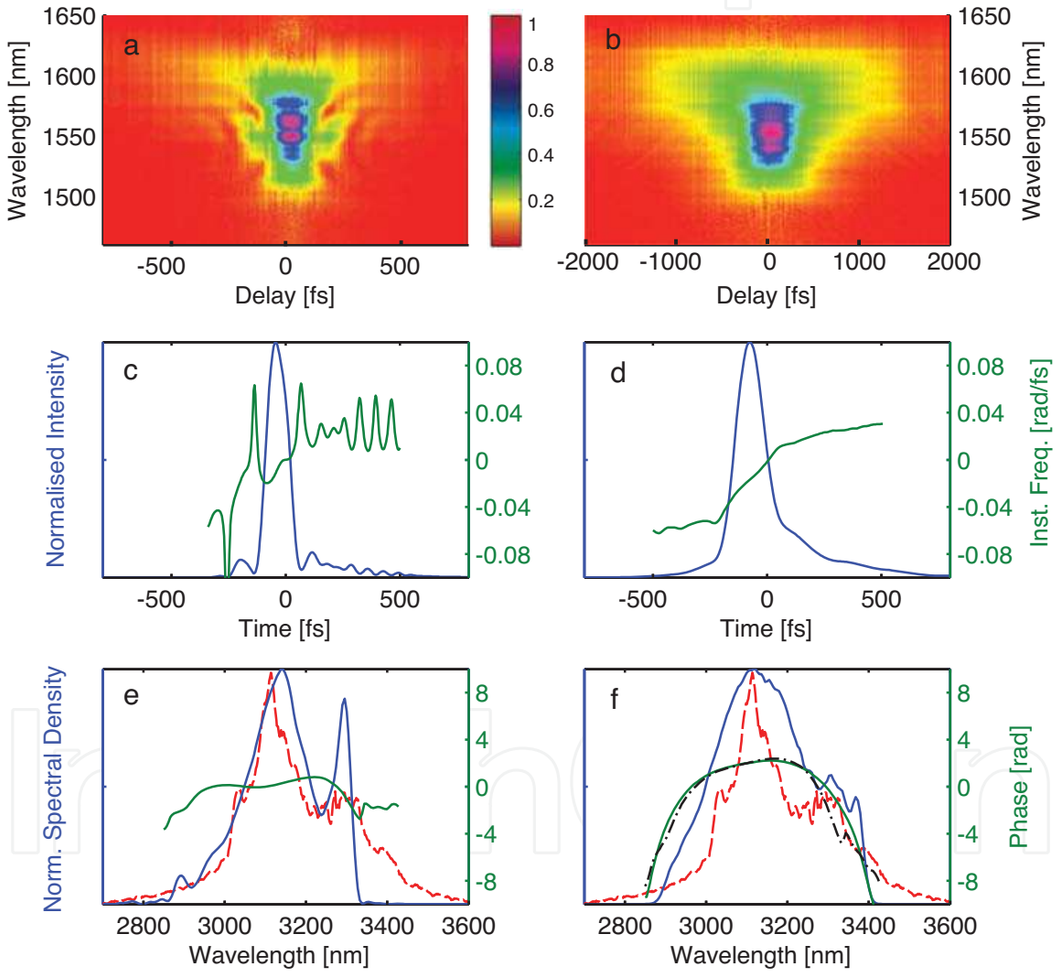

Fig. 10. **(a)** FROG trace of undispersed pulse - colour shows the square root of intensity. **(b)** FROG trace after propagation through 1 cm sapphire (note different timescale). **(c)** Retrieved intensity and instantaneous frequency (right scale) from **a**. **(d)** Retrieved intensity and instantaneous frequency from **b**. **(e)** Retrieved (solid) & measured (dashed) spectrum (left scale) and spectral phase (right scale) of unchirped pulse. **(f)** Retrieved & measured spectrum and spectral phase after 1 cm sapphire. The dash-dot line shows the calculation of the expected spectral phase

can see that there is good agreement - the overall shape is accurately retrieved and the deviation of the spectral phase is less than a radian from 2850-3270 nm. We note that calculation of the phase in this region is difficult due to lack of reliable values for material refractive indices, and further the difference in the temporal domain from the calculated and measured phases corresponds to just over half an optical cycle, or 5.4 fs.

4.1 Stability

We monitored the power of the compressed pulse over half an hour by sending the full beam onto a pyroelectric detector from OPHIR (3A head, acquisition rate 3Hz) and measured a power stability of 0.75% RMS over 30 minutes - see also Fig. 11. The stability is excellent and - to our knowledge - signifies the lowest jitter observed from any OPCPA system, which exhibit from 1.5% RMS fluctuations and higher (Tavella et al. (2010); Ishii et al. (2005)). We note that our measurement represents a low-pass filtered result due to the inadequate response times of the detector, especially for the 100 kHz repetition rate. Such an analysis is analog to most measurements quoted in the literature but higher peak to peak fluctuations might exist which we plan to investigate in a future measurement. The inset in Fig. 11 shows a knife edge measurement of the compressed pulse and the high spatial quality, which is sufficient for focussing close to the diffraction limit.

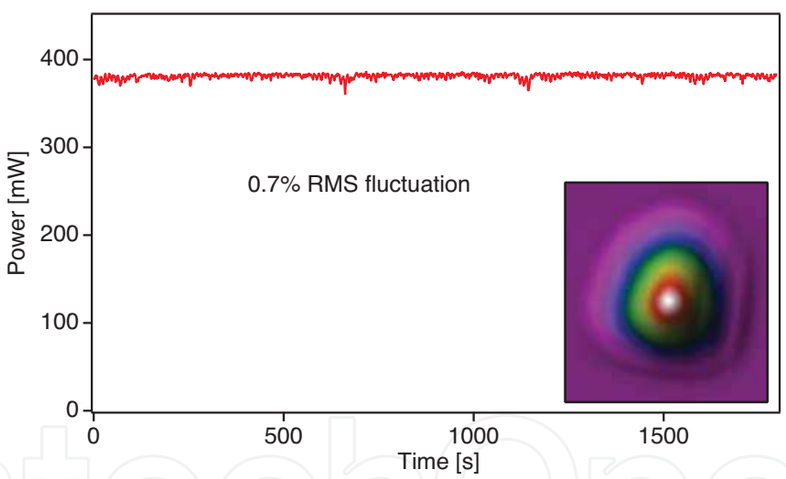

Fig. 11. **Stability of the system and profile.** The stability of the OPCPA system after compression is excellent with fluctuation under 0.75% over 30 minutes. Insert is the beam profile after compression

5. Conclusion

Sources of ultrashort pulses in the mid-IR are in high demand, as can be seen from the many examples we have presented here, from a range of very different fields: life sciences to strong field physics. OPCPA is a technique which frees many operating parameters from the restrictions of the current CPA based systems. We have, as example, presented a source which is capable of satisfying the needs of a wide variety of fields: some require high repetition rate, others few cycle pulses, yet others CEP stability, while strong field physics

ideally needs all of these features combined. This system currently signifies the highest energy shortest pulse OPCPA system in the mid-IR with compressed pulse energy of 3.8 μJ at 100 kHz, a pulse duration of 67 fs (6.3 cycles) and a central wavelength at 3.2 μm. This system is in principle CEP stable, and offers an important proof of principle, showing that OPCPA can be used to operate at extremely high average powers in the mid-IR.

We have also described a broad-bandwidth, high resolution SHG-FROG device, for few-cycle pulse measurement in the mid-IR. The system is capable of measuring pulses over a wide wavelength range spanning from 800 nm to 5 μm and for large temporal ranges up to 100 ps. This system has been used to measure a complex sub-10-cycle (sub-100-fs) mid-IR pulse and also to retrieve the change introduced in a ~100 fs mid-IR pulse by the dispersion of a sapphire plate. The retrieved and experimental FROG traces show rich detail and excellent agreement. The ability to characterise few-cycle mid-IR laser pulses is a pre-requisite not only for optimization of such laser systems, but also for the application of ultrashort mid-IR pulses to experiments in the described wide range of fields.

Ultrafast pulsed light sources in the mid-IR have a very bright future, due to growing interest in this area combined with a growing range of applications. We have presented here a prototype for the next generation of ultrashort mid-IR sources. Our novel source, with its combination of passively stabilised CEP and broad bandwidth OPCPA, provides an ideal template for the development of high energy, high repetition rate mid-IR systems. The use of OPCPA should in the near future allow the production of few-cycle pulse durations without the need for nonlinear broadening, while the high rep rate and stability already are ideal for ultrafast spectroscopy. OPCPA is a scaleable technique, and the pulses from this system could easily be increased to mJ level at lower repetition rates, by including additional OPCPA stages pumped by high energy, commercially available pump lasers. The availability of such sources will open up a new regime of strong field and spectroscopic experiments driven by mid-IR pulses.

6. References

Qian Peng, Asta Juzeniene, Jiyao Chen, Lars O Svaasand, Trond Warloe, Karl-Erik Giercksky, and Johan Moan. Lasers in medicine. *Reports on Progress in Physics*, 71(5):056701, 2008.

A. Mcpherson, G. Gibson,H. Jara, U. Johann, T. S. Luk, I. Mcintyre, K. Boyer, and C. K. Rhodes. Studies of multiphoton production of vacuum-ultraviolet radiation in the rare gases. *J. Opt. Soc. Am. B*, 4:595, 1987.

M. Ferray, A. L'Huillier, X. F. Li, L. A. Lompr, G. Mainfray, and C. Manus. Multiple-harmonic conversion of 1064 nm radiation in rare gases. *J. Phys. B*, 21:L31–L35, 1988.

B Sheehy, J.d.d.Martin, L. F. Dimauro, P Agostini, K. J. Schafer, M Gaarde, and K. C. Kulander. High harmonic generation at long wavelengths. *Phys. Rev. Lett.*, 83:5270, 1999.

A. Gordon and F.X. Kaertner. Scaling of kev hhg photon yield with drive wavelength. *Opt. Exp.*, 13(8):2941–2947, 2005.

J. Tate, T. Auguste, H. G. Muller, P. Salieres, P. Agostini, and L. F. DiMauro. Scaling of wave-packet dynamics in an intense midinfrared field. *Physical Review Letters*, 98(1):013901, January 2007.

Tenio Popmintchev, Ming-Chang Chen, Oren Cohen, Michael E. Grisham, Jorge J. Rocca, Margaret M. Murnane, and Henry C. Kapteyn. Extended phase matching of high harmonics driven by mid-infrared light. *Opt. Lett.*, 33(18):2128–2130, 2008.

R. Moshammer, M Unverzagt, W Schmitt, J Ullrich, and H Schmidt-Bocking. A 4 pi recoil-ion electron momentum analyzer: a high-resolution ″microscope″ for the investigation of the dynamics of atomic, molecular and nuclear reactions. *Nuc. Instrum. Meth. Phys. Res. Sec. B*, 108(4):425–445, 1996.

M. J. Thorpe and J. Ye. Cavity-enhanced direct frequency comb spectroscopy. *Applied Physics B-Lasers And Optics*, 91(3-4):397–414, June 2008.

M Nisoli, S Stagira, S De Silvestri, O Svelto, S Sartania, Z Cheng, G Tempea, C Spielmann, and F Krausz. Toward a terawatt-scale sub-10-fs laser technology. *IEEE J. Sel. Top. Quant. Electron.*, 4(2):414–420, 1998.

C.P. Hauri, W. Kornelis, F.w. Helbing, a. Heinrich, a. Couairon, a. Mysyrowicz, J. Biegert, and U. Keller. Generation of intense, carrier-envelope phase-locked few-cycle laser pulses through filamentation. *Appl. Phys. B*, 79(6):673–677, 2004.

B Schenkel, J Biegert, U Keller, C Vozzi, M Nisoli, G Sansone, S Stagira, S De Silvestri, and OSvelto. Generation of 3.8-fs pulses froma daptive compression of a cascaded hollow fiber supercontinuum. *OPTICS LETTERS*, 28(20):1987–1989, OCT 15 2003.

T. Wilhelm, J. Piel, and E. Riedle. Sub-20-fs pulses tunable across the visible from a blue-pumped single-pass noncollinear parametric converter. *Opt. Lett.*, 22(19):1494–1496, 1997.

Christian Schriever, Stefan Lochbrunner, Patrizia Krok, and Eberhard Riedle. Tunable pulses from below 300 to 970 nm with durations down to 14 fs based on a 2 mhz ytterbiumdoped fiber system. *Opt. Lett.*, 33(2):192–194, 2008.

C. Vozzi, G. Cirmi, C. Manzoni, E. Benedetti, F. Calegari, G. Sansone, S. Stagira, O. Svelto, S. De Silvestri, M. Nisoli, and G. Cerullo. High-energy, few-optical-cycle pulses at 1.5 mu m with passive carrier-envelope phase stabilization. *Optics Express*, 14(21): 10109–10116, October 2006.

G. Cirmi, C.Manzoni, D. Brida, S. De Silvestri, and G. Cerullo. Carrier-envelope phase stable, few-optical-cycle pulses tunable from visible to near ir. *Journal Of The Optical Society Of America B-Optical Physics*, 25(7):B62–B69, July 2008.

Chunmei Zhang, Pengfei Wei, Yansui Huang, Yuxin Leng, Yinghui Zheng, Zhinan Zeng, Ruxin Li, and Zhizhan Xu. Tunable phase-stabilized infrared optical parametric amplifier for high-order harmonic generation. *Opt. Lett.*, 34(18):2730–2732, 2009.

D. Brida, M. Marangoni, C. Manzoni, S. De Silvestri, and G. Cerullo. Two-optical-cycle pulses in the mid-infrared from an optical parametric amplifier. *Optics Letters*, 33(24):2901– 2903, December 2008.

Erik T. J. Nibbering and Thomas Elsaesser. Ultrafast vibrational dynamics of hydrogen bonds in the condensed phase. *Chemical Reviews*, 104(4):1887–1914, April 2004.

F. Rotermund, V. Petrov, F. Noack, M. Wittmann, and G. Korn. Laser-diode-seeded operation of a femtosecond optical parametric amplifier with mgo:linbo3 and generation of 5- cycle pulses near 3 μm. *J. Opt. Soc. Am. B*, 16(9):1539–1545, 1999.

T. Fuji, N. Ishii, C. Y. Teisset, X. Gu, T. Metzger, A. Baltuska, N. Forget, D. Kaplan, A. Galvanauskas, and F. Krausz. Parametric amplification of few-cycle carrier-envelope phase-stable pulses at 2.1 mu m. *Optics Letters*, 31(8):1103–1105, April 2006.

S. Adachi, N. Ishii, T. Kanai, A. Kosuge, J. Itatani, Y. Kobayashi, D. Yoshitomi, K. Torizuka, and S. Watanabe. 5-fs, multi-mj, cep-locked parametric chirped-pulse amplifier pumped by a 450-nm source at 1 khz. *Optics Express*, 16(19):14341–14352, September 2008.

O. Chalus, P. K. Bates, M. Smolarski, and J. Biegert. Mid-ir short-pulse opcpa with micro-joule energy at 100 khz. *Optics Express*, 17(5):3587–3594, March 2009.

O. V. Chekhlov, J. L. Collier, I.N. Ross, P. K. Bates, M. Notley, C. Hernandez-Gomez, W. Shaikh, C. N. Danson, D. Neely, P. Matousek, and S. Hancock. 35 j broadband femtosecond optical parametric chirped pulse amplification system. *Optics Letters*, 31(24):3665– 3667, December 2006.

V. V. Lozhkarev, G. I. Freidman, V. N. Ginzburg, E. V. Katin, E. A. Khazanov, A. V. Kirsanov, G. A. Luchinin, A. N. Mal'shakov, M. A. Martyanov, O. V. Palashov, A. K. Poteomkin, A. M. Sergeev, A. A. Shaykin, I. V. Yakovlev, S. G. Garanin, S. A. Sukharev, N. N. Rukavishnikov, A. V. Charukhchev, R. R. Gerke, and V. E. Yashin. 200 tw 45 fs laser based on optical parametric chirped pulse amplification. *Optics Express*, 14(1):446– 454, January 2006.

M. Gertsvolf, H. Jean-Ruel, P. P. Rajeev, D. D. Klug, D. M. Rayner, and P. B. Corkum. Orientation-dependent multiphoton ionization in wide band gap crystals. *Phys. Rev. Lett.*, 101(24):243001, Dec 2008.

F. Tavella, A. Willner, J. Rothhardt, S.Hädrich, E. Seise, S. D¨usterer, T. Tschentscher, H. Schlarb, J. Feldhaus, J. Limpert, A. Tünnermann, and J. Rossbach. Fiber-amplifier pumped high average power few-cycle pulse non-collinearopcpa. *Opt. Express*, 18(5):4689– 4694, 2010.

N. Ishii, L. Turi, V. S. Yakovlev, T. Fuji, F. Krausz, A. Baltuska, R. Butkus, G. Veitas, V. Smilgevicius, R. Danielius, and A. Piskarskas. Multimillijoule chirped parametric amplification of few-cycle pulses. *Optics Letters*, 30(5):567–569, March 2005.

F. Roser, J. Rothhard, B. Ortac, A. Liem, O. Schmidt, T. Schreiber, J. Limpert, and A. Tunnermann. 131 w 220 fs fiber laser systems. *Optics Letters*, 30(20):2754–2756, October 2005.

Johan Boullet, Yoann Zaouter, Jens Limpert, Stéphane Petit, Yann Mairesse, Baptiste Fabre, Julien Higuet, Eric Mével, Eric Constant, and Eric Cormier. High-order harmonic generation at a megahertz-level repetition rate directly driven by an ytterbium-doped- fiber chirped-pulse amplification system. *Opt. Lett.*, 34(9):1489–1491, 2009.

A Baltuska, T Fuji, and T Kobayashi. Controlling the carrier-envelope phase of ultrashort light pulses with optical parametric amplifiers. *Phys. Rev. Lett.*, 88(13):133901, 2002.

A. Renault, D. Z. Kandula, S. Witte, A. L. Wolf, R. T. Zinkstok, W. Hogervorst, and K. S. E. Eikema. Phase stability of terawatt-class ultrabroadband parametric amplification. *Optics Letters*, 32(16):2363–2365, August 2007.

F. Adler, A. Sell, F. Sotier, R. Huber, and A. Leitenstorfer. Attosecond relative timing jitter and 13 fs tunable pulses froma two-branch er: fiber laser. *Optics Letters*, 32(24):3504–3506, December 2007.

O. Chalus, P. K. Bates, and J. Biegert. Design and simulation of few-cycle optical parametric chirped pulse amplification at mid-ir wavelengths. *Optics Express*, 16(26):21297–21304, December 2008.

Jeffrey Moses, Cristian Manzoni, Shu-Wei Huang, Giulio Cerullo, and Franz X. Kaertner. Temporal optimization ofultrabroadband high-energy opcpa. *Opt. Express*, 17(7):5540– 5555, 2009.

C. Y. Teisset, N. Ishii, T. Fuji, T. Metzger, S. Kohler, R. Holzwarth, A. Baltuska, A.M. Zheltikov, and F. Krausz. Soliton-based pump-seed synchronization for few-cycle opcpa. *Optics Express*, 13(17):6550–6557, AUG 22 2005.

S. Witte, R. T. Zinkstok, W. Hogervorst, and K. S. E. Eikema. Generation of few-cycle terawatt light pulses using optical parametric chirped pulse amplification. *Optics Express*, 13 (13):4903–4908, Jun 27 2005.

I. N. Ross, G. H. C. New, and P. K. Bates. Contrast limitation due to pump noise in an optical parametric chirped pulse amplification system. *Optics Communications*, 273(2):510– 514, May 2007.

F. Tavella, K. Schmid, N. Ishii, A. Marcinkeviius, L. Veisz, and F. Krausz. High-dynamic range pulse-contrast measurements of a broadband optical parametric chirped-pulse amplifier. *Applied Physics B: Lasers and Optics*, 81(6):753–756, October 2005.

M. Kakehata, H. Takada, Y. Kobayashi, K. Torizuka, H. Takamiya, K. Nishijima, T. Homma, H. Takahashi, K. Okubo, S. Nakamura, and Y. Koyamada. Carrier-envelope-phase stabilized chirped-pulse amplification system scalable to higher pulse energies. *Optics Express*, 12(10):2070–2080, May 2004.

R. Trebino. *Frequency-Resolved Optical Gating*. Kluwer Academic Publishers, 2000. C. Iaconis and I. A. Walmsley. Spectral phase interferometry for direct electric-field reconstruction of ultrashort optical pulses. *Optics Letters*, 23(10):792–794, May 1998.

T. Fuji and T. Suzuki. Generation of sub-two-cycle mid-infrared pulses by four-wave mixing through filamentation in air. *Optics Letters*, 32(22):3330–3332, November 2007.

D. GRISCHKOWSKY, S. KEIDING, M. VANEXTER, and C. FATTINGER. Far-infrared time-domain spectroscopy with terahertz beams of dielectrics and semiconductors. *Journal Of The Optical Society Of America B-Optical Physics*, 7(10):2006–2015, October 1990.

K. NAGANUMA, K. MOGI, and H. YAMADA. General-method for ultrashort light-pulse chirp measurement. *Ieee Journal Of Quantum Electronics*, 25(6):1225–1233, June 1989.

W. Kornelis, J. Biegert, J. W. G. Tisch, M. Nisoli, G. Sansone, C. Vozzi, S. De Silvestri, and U. Keller. Single-shot kilohertz characterization of ultrashort pulses by spectral phase interferometry for direct electric-field reconstruction. *Optics Letters*, 28(4):281–283, February 2003.

K. W. DELONG, C. L. LADERA, R. TREBINO, B. KOHLER, and K. R. WILSON. Ultrashortpulse measurement using noninstantaneous nonlinearities - raman effects in frequency-resolved optical gating. *Optics Letters*, 20(5):486–488, March 1995.

Selcuk Akturk, Mark Kimmel, and Rick Trebino. Extremely simple device for measuring 1.5 micron ultrashort laser pulses. *Opt. Express*, 12(19):4483–4489, 2004.

B. A. Richman, M. A. Krumbugel, and R. Trebino. Temporal characterization of mid-ir free-electron-laser pulses by frequency-resolved optical gating. *Optics Letters*, 22(10):721– 723, May 1997.

A. Smith. Snlo version 5.0, nonlinear optics code. available from A.V. Smith, AS-Photonics, Albuquerque, N.M., 2009.

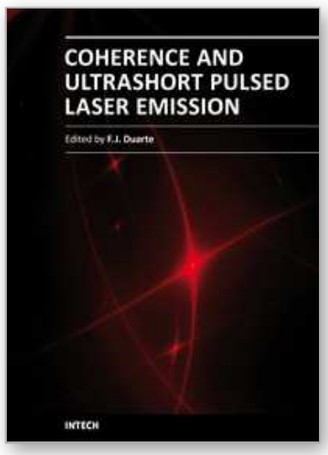

Coherence and Ultrashort Pulse Laser Emission

Edited by Dr. F. J. Duarte

ISBN 978-953-307-242-5
Hard cover, 688 pages
Publisher InTech
Published online 30, November, 2010
Published in print edition November, 2010

In this volume, recent contributions on coherence provide a useful perspective on the diversity of various coherent sources of emission and coherent related phenomena of current interest. These papers provide a preamble for a larger collection of contributions on ultrashort pulse laser generation and ultrashort pulse laser phenomena. Papers on ultrashort pulse phenomena include works on few cycle pulses, high-power generation, propagation in various media, to various applications of current interest. Undoubtedly, Coherence and Ultrashort Pulse Emission offers a rich and practical perspective on this rapidly evolving field.

INTECH
open science | open minds

InTech Europe
University Campus STeP Ri
Slavka Krautzeka 83/A
51000 Rijeka, Croatia
Phone: +385 (51) 770 447
Fax: +385 (51) 686 166
www.intechopen.com

InTech China
Unit 405, Office Block, Hotel Equatorial Shanghai
No.65, Yan An Road (West), Shanghai, 200040, China
中国上海市延安西路65号上海国际贵都大饭店办公楼405单元
Phone: +86-21-62489820
Fax: +86-21-62489821

IntechOpen